



Evaluation of the influence of the formalin fixation time on the elemental content of tissues measured with X-ray fluorescence

Sofia Pessanha^{a,b,*}, Alexandre Veiga^a, Delfim Doutel^{c,d}, Fernanda Silva^c, João Silva^a,
Patrícia M. Carvalho^{a,b}, Sofia Barbosa^{a,e}, José Paulo Santos^{a,b}, Ana Félix^{c,d}, Jorge Machado^{a,b}

^a NOVA School of Science and Technology, Campus Caparica, 2829-516 Caparica, Portugal

^b LIBPhys, Laboratory of Instrumentation, Biomedical Engineering and Radiation Physics, FCTUNL, 2829-516, Caparica, Portugal

^c NOVA Medical School, Campo dos Mártires da Pátria 130, 1169-056 Lisboa, Portugal

^d Instituto Português de Oncologia de Lisboa Francisco Gentil (IPOLFG), rua Professor Lima Basto, 1099-023, Lisboa, Portugal

^e GeoBioTec, Campus Caparica, 2829-516 Caparica, Portugal

ARTICLE INFO

Keywords:

Formalin fixation
Human tissues
EDXRF
Quantification

ABSTRACT

One of the most widely used methods for tissue preservation and fixative during transportation is the conservation in formalin during variable amounts of time. In this study, we have evaluated the influence of formalin fixation time in the elemental composition of human tissue samples using Energy Dispersive X-Ray Fluorescence (EDXRF).

Ten sets of human tissue samples (from colon, ileum, stomach, and spleen) were exposed to different formalin fixation times, between 2 and 24 days, and for each tissue, the elemental content throughout time was compared to the elemental content of the snap-frozen sample of the same tissue that was not exposed to formalin. Additionally, in order to further evaluate the transference of elements, the formalin solution was also analysed using EDXRF.

Our results showed a clear decrease of Cl and K in the tissues, transferred to the formalin solution. Conversely, there is an uptake of P in the tissue, likely due to the buffered formalin solution. The consistent alterations seen in the studied elements across all the ten different tissues allow us to hypothesize that in the future, there will be different thresholds for their use as diagnostic tools in unfixed (intraoperative exams) as well as formalin fixed paraffin embedded tissues.

1. Introduction

Tissue homeostasis requires suitable performance of cellular processes, which depend not only on RNA and proteins, but also on inorganic elements that serve as their cofactors [1]. For instance, Cu and Zn are essential components or cofactors of hundreds of enzymes, while antioxidant enzymes, such as glutathione peroxidases, also require the presence of manganese as an essential cofactor [2]. Studies have shown that available Fe plays an important role in cell growth regulation and induces oxidative stress, causing DNA, protein, and organelle damage, through the production of reactive oxygen species [3,4]; Ca is involved in many cellular processes, such as, apoptosis, gene transcription, and angiogenesis [5].

As the understanding of the mechanisms of assimilation/accumulation of major (over 100 µg/g) [6] and trace (over 10 µg/g) [6] elements

may be indicative of the genesis or progression of certain diseases, several analytical techniques have been essayed in biomedical applications, namely, X-Ray Fluorescence methods [7–9], Ion Beam Analysis [10,11], Inductively Coupled Plasma techniques [12,13], and Neutron Activation Analysis [14,15]. These techniques have been applied to human biopsied samples, [7,16] cadavers [9,13], and euthanized model animals [12,17]. Regardless of the sample preparation that each technique requires, ranging from direct analysis to cryo-sectioning or sample's acidic digestion, sample preservation between collection and analysis must be ensured.

Although the samples can be snap-frozen [16,18,19], preserved with solutions, such as deionized water [15,20], or sealed in vacuum, the most widely used method for tissue preservation and fixative during transportation between hospital departments is the conservation in formalin during variable amounts of time [3,17,21–23].

* Corresponding author at: NOVA School of Science and Technology, Campus Caparica, 2829-516 Caparica, Portugal.

E-mail address: sofia.pessanha@fct.unl.pt (S. Pessanha).

<https://doi.org/10.1016/j.sab.2023.106704>

Received 16 September 2022; Received in revised form 4 May 2023; Accepted 8 May 2023

Available online 9 May 2023

0584-8547/© 2023 The Authors. Published by Elsevier B.V. This is an open access article under the CC BY-NC-ND license (<http://creativecommons.org/licenses/by-nc-nd/4.0/>).

Moreover, if there is a need to study Formalin-Fixed Paraffin Embedded (FFPE) tissue blocks stored in medical centres, one must account for the formalin fixation period of the tissues before embedding [1,13,24–29]. Although the effect of freezing the samples has been considered innocuous [30], information regarding the impact of the formalin fixation time and the elemental concentrations is scarce. Chwiej et al. [31] reported variations of the mass per unit area of some elements in rat brain sample after perfusion and immersion in formalin, that were attributed to shrinkage or swelling of the tissue. This effect was described by Quester and Schröder [32] in brain after an average of 70 days of formalin fixation.

Compared to other atomic spectrometry techniques, Energy Dispersive X-Ray Fluorescence (EDXRF) constitutes the ideal compromise of non-destructive nature, simple instrumentation, and good sensitivity for the elements of interest ($Al = 13 < Z < 83 = Bi$). For these reasons, this technique has already been tested in the quantitative analysis of human tissues, from the toxicological assessment of hair and nail clippings [33] to the characterization and imaging of brain tissues presenting neurodegenerative diseases [34], as well as the comparison to adjacent normal healthy tissue and tumor colon [3,21] and lung [3,35] samples.

Elemental quantification using EDXRF is commonly performed using the Fundamental Parameter (FP) method, an iterative approach that estimates a composition for the unknown sample by calculating its theoretical fluorescence intensities (considering both elements and matrix) and comparing them with the measured ones, until a correspondence is obtained [36]. The uncertainty associated with the method increases when the constituent elements of the matrix are not detectable by EDXRF (typically H, C, O and N for biological samples), but significantly influences how the remaining elements of interest are detected. Ensina et al. [8] have essayed different combinations of those elements to determine a suitable matrix (provided ad hoc to the FP-method software) for freeze-dried and pelletized biological tissues, reaching a good compromise in accuracy for both light and heavier elements when setting the dark matrix at 10% - H, 22% - C, 3% - N, and 60% - O.

In this work, we will gauge the variation of trace element concentration in human tissues subjected to different formalin fixation times. Although concern regarding human exposure to this chemical has increased and regulation has been implemented, the benefits of its use in biomedical applications have always been assumed. However, it is of paramount importance to any researcher investigating the influence of elemental content in tissues (both human and animal) to know the limitations of the use of this solution. In order to evaluate and quantify this influence, we will determine the elemental content of 10 sets of human tissue samples (from colon, ileum, stomach, and spleen) using EDXRF. Each set of samples will be exposed to different formalin fixation times, between 2 days and two weeks – normal time spend considered for FFPE sample preparation procedure; and a prolonged time of 23–24 days – considering samples that were collected from medical facilities but were not analysed in a timely fashion due to instrumentation/sample preparation constraints or the previewed time for clinicians raised question after receiving the final pathological report before the elimination of human samples. For each tissue, the elemental content throughout time was compared to the elemental content of the snap-frozen sample of the same tissue that was not exposed to formalin.

2. Materials and methods

2.1. Human tissues

Samples were obtained from Instituto Português de Oncologia de Lisboa, Francisco Gentil (IPOLFG). Every tissue sample was collected from different patients that have signed an informed consent to authorize their collection for research. This specific study was authorized and approved by the Ethics Committee of IPOLFG (UIC/1417), and all experiments were performed under the guidelines and regulations for handling human tissues. Samples (cold ischemia <10 min) were

collected from 10 surgical specimens and divided into cubes with approximately 1 cm^3 . Colon samples were washed when there was suspicion of faecal contamination. Only adjacent normal healthy tissue was selected for this research, hence, the amount of obtainable tissue was scarce: depending on the available amount of tissue, sets of 2 to 6 portions from each specimen were obtained. One portion of each set was snap-frozen, and the remaining portions were preserved in a 10% v/v formalin buffered solution (4% formaldehyde stabilised with methanol 0.5–1.5%, VMR Chemicals, USA) until removal from the vials, according to different time-frames, between 2 and 24 days.

Samples were removed from the vials, washed with distilled water to remove excess formalin, and freeze-dried using a Modulyo Freeze Dryer system (Edwards, UK), operated at $-60 \text{ }^\circ\text{C}$ and 20 Pa. Total freeze-drying time was different among samples, for example colon samples, due to larger quantities of adipose tissue, took longer time to lyophilize.

The lyophilized samples were powdered using a pestle and mortar, and a mechanical mill. The obtained powder was pressed into pellets, 1.1–1.2 mm thick, that were glued onto a Mylar film and placed on a slide frame. Each tissue cube rendered only one pellet.

2.2. Experimental setup – micro-energy dispersive X-ray fluorescence system

EDXRF analysis of the samples was performed with a benchtop micro energy dispersive X-ray fluorescence (μ -EDXRF) system, the M4 TORNADO (Bruker, Germany). This spectrometer system uses poly-capillary X-ray optics with spot size of $25 \text{ }\mu\text{m}$ for Mo – $K\alpha$ radiation. The excitation of samples is achieved with a peltier-cooled X-ray tube with a Rh target, and the detection is achieved with a silicon drift detector (SDD) that has a sensitive area of 30 mm^2 and energy resolution 145 eV for the $K\alpha$ line of Mn. The X-ray tube was operated at 50 kV, 300 μA , $12.5 \text{ }\mu\text{m}$ Al filter, and 20 mBar vacuum inside the system's chamber.

2.3. Quantification method and validation

2.3.1. Human tissues

Elemental quantification of the analysed pellets was performed using MQuant, an in-built software of the M4 TORNADO system. It allows spectra deconvolution, peak fitting, and quantification using the Fundamental Parameters (FP) method based on Sherman's equation [37]. The uncertainty associated with the method increases when the constituent elements of the matrix are not detectable by EDXRF, (typically H, C, O and N for biological samples), but significantly influences how the remaining elements of interest are detected. Considering Ensina et al. [8], the following matrix composition, was considered suitable: 10% - H, 22% - C, 3% - N, and 60% - O and provided ad-hoc to the software.

Limits of Detection (LoD) [38], Limits of Quantification (LoQ) [38], and validation results for the reference material Oyster Tissue SRM 1566 were determined and are presented in supplementary material (Fig. S1 (Appendix) and Table S1 (Appendix)). Bias was calculated as: Bias [%] = (experimental value - certified value/certified value) x 100 [12]. A higher bias was determined for Zn, most likely because for this element the infinitely thick sample criterion is not fully met [36]. However, all samples, CRM and unknowns were prepared in the same way. To ensure that the analysis was as representative as possible of the composition of the samples and to surpass the issue of the heterogeneity of the pellets, three $6 \times 6 \text{ mm}^2$ area acquisitions were performed and quantitative results obtained from each cumulative spectrum. The scans were performed with a $35 \text{ }\mu\text{m}$ step and a time per step of 12 ms/pixel, yielding an acquisition time of, approximately, 7 min.

2.3.2. Formalin retainer filters

To evaluate the transference of elements to and from the formalin solution, 200 μL of formalin from each container were pipetted to paper filter retainers, microcarry (Rigaku, Japan), following the methodology

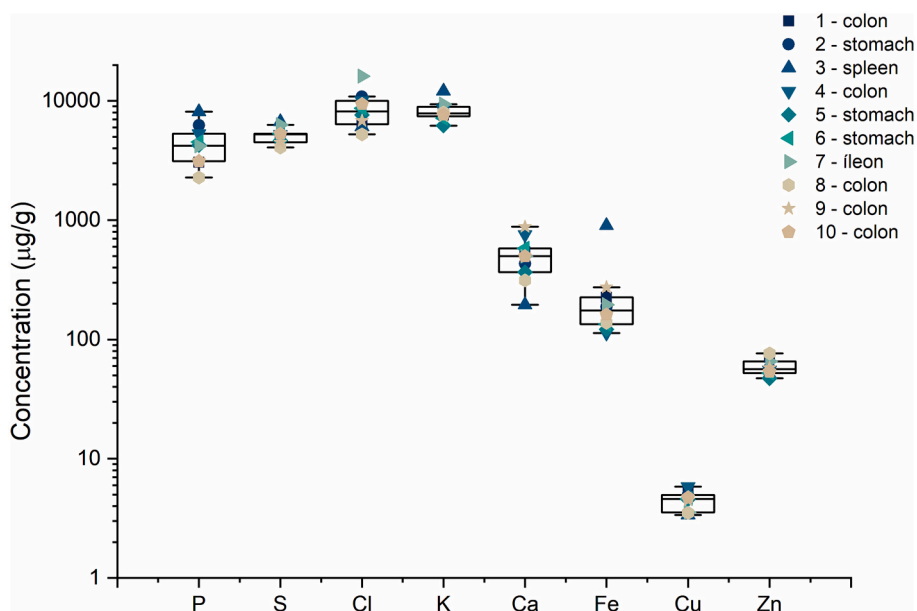


Fig. 1. Box-plot charts of the elemental concentration distribution ($\mu\text{g/g}$) of P, S, Cl, K, Ca, Fe, Cu and Zn for the different snap-frozen samples. The box (interquartile range (from 25th to 75th percentiles) overlaps with the data in order to gauge distribution. Open squares represent the mean value of element concentration, black line in each box represents median while whiskers are ranges from 10th to 90th percentiles.

developed for the analysis of liquids samples using EDXRF [39]. Area scans ($21 \times 21 \text{ mm}^2$) were performed in order to encompass the whole filter area - scans were performed with a $35 \mu\text{m}$ step and a time per step of 12 ms/pixel, yielding an acquisition time of, approximately, 40 min. Using a tool from MQuant software, circumferences with 20 mm diameter were selected and the corresponding spectrum was saved (Fig. S2 (Appendix)).

Quantification of the paper retainer filters was performed with empirical calibration curves (see supplementary table S2), using the following leaves Certified Reference Materials (CRM), whose matrix is cellulose: bush branches and leaves GBW 07603, poplar leaves GBW 07604, orchard leaves NBS1571, and tea leaves GBW 07605). About 0.1 g of powder of each standard reference material was pressed into a 20 mm diameter \times 0.7 mm thickness pellets and an acquisition procedure similar to the paper filters was performed.

This procedure has been previously applied to ancient documents by Manso et al [40] The method's accuracy was assessed using a sample of Whatman paper for conservation purposes, of known concentration [41], and the results are present in supplementary material Table S3 (Appendix).

2.4. Statistical analysis

Statistical evaluation of the significance of the differences between formalin fixation times was performed by means of k-means cluster analysis using OriginPro® software.

3. Results and discussion

Fig. 1 summarizes the obtained elemental concentrations in the 10 snap-frozen samples. The results for each sampling point (corresponding to a given period of time in formalin) are presented as box and whiskers plots: the box (interquartile range - from 25th to 75th percentiles) overlaps with the data in order to gauge distribution, open squares represent the mean value of element concentration, the black line in each box represents the median, and whiskers are ranges from 10th to 90th percentiles. This distribution shows the concentration ranges of major and trace elements obtained for the different samples.

The obtained values were compared against values found in

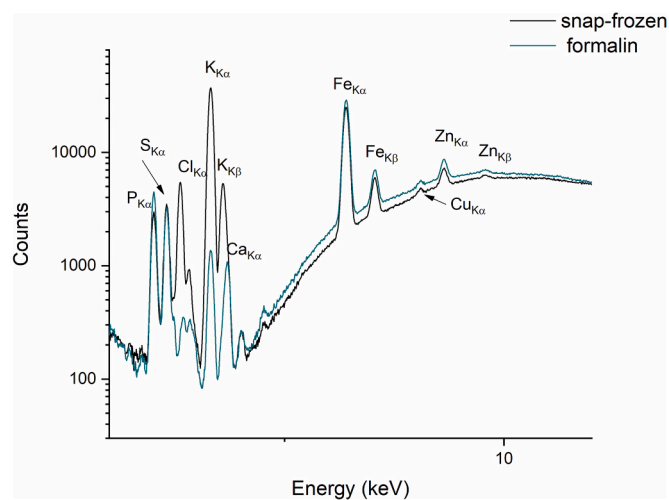


Fig. 2. Comparison of the spectra obtained for snap-frozen then lyophilized tissue and after 6 days formalin fixation.

literature (Table 2) from TXRF, EDXRF, NAA, and PIXE analyses. Research found on colon, stomach, and spleen was scarce and for ileum, to the best of our knowledge, non-existent. As reference for the order of magnitude, levels found on other organs, such as, breast, prostate, uterus, and thyroid, were added to the table (other tissues). As can be seen, the concentrations of all elements, determined in snap-frozen samples, fall within the expected ranges. For most elements, the elemental variation is small: except for P, Cl, and Ca, for which the order of magnitude does not vary between the analysed tissues. Regarding Ca, the concentration varies between $190 \pm 7 \mu\text{g/g}$ in spleen and $880 \pm 7 \mu\text{g/g}$ in colon sample #9, values well within the ranges presented in Table 2. Phosphorus concentration was found to be between $2300 \pm 100 \mu\text{g/g}$ in colon sample #8 and $8130 \pm 50 \mu\text{g/g}$ in spleen. Despite Cl being scarcely evaluated, it is clearly present in major concentrations. We highlight the case of Fe in spleen samples, presenting a mean concentration value of $901 \pm 3 \mu\text{g/g}$, much higher than the values reported in literature, with exception of the value determined by Mulware et al.

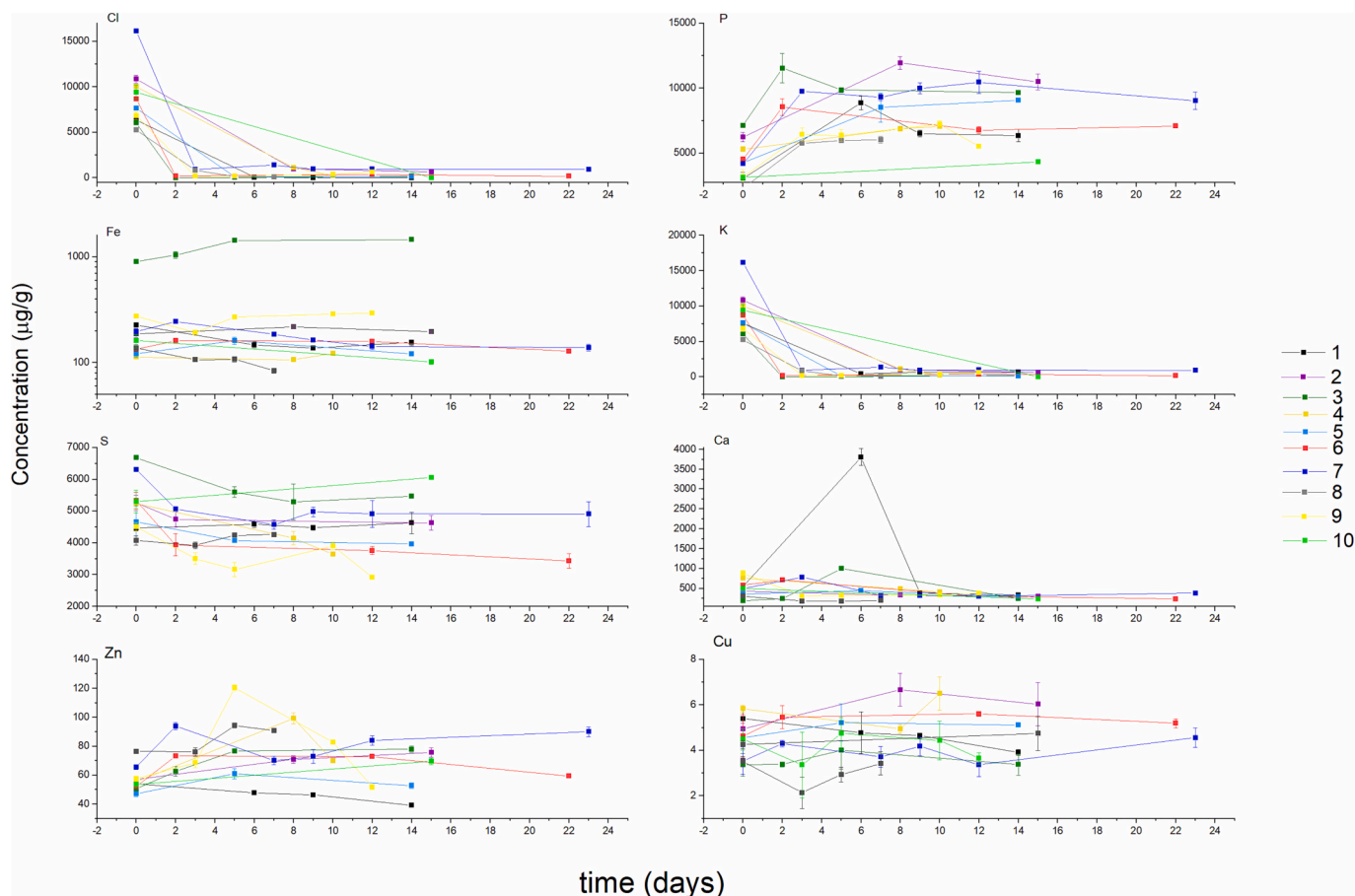


Fig. 3. Variation of Potassium, Chlorine, Calcium, Phosphorus, Sulphur, Iron, Copper and Zinc mean concentrations ($\mu\text{g/g}$) in tissues with time in formalin. Error bars correspond to the maximum deviation to the mean.

[18] in stomach.

Fig. 2 presents the comparison of EDXRF spectra obtained for a snap-frozen lyophilized tissue and lyophilized tissue after 6 days in formalin. As can be seen, the decrease of K and Cl after formalin fixation is remarkable.

Figs. 3 depict the variation of the mean concentrations of P, S, Cl, K, Ca, Fe, Cu and Zn, for each sample set, with time preserved in formalin. Error bars correspond to the maximum deviation to the mean for the three replicas of each sample. As can be seen in Fig. 3, there is a sharp decrease of the concentrations of K and Cl after the first period of fixation in formalin. Afterwards, the concentration values remain constant. Regarding Cl, the decrease in concentration ranged from 91% in sample set #2, after eight days in formalin, to 99% for sample set #3, after two days in formalin. Similarly, for K, the decrease ranged from 76% in sample set #4, after eight days in formalin, to 97% in sample set #10, after fifteen days in formalin. In sample set #7, after two days in

Table 1

Description of the analysed tissues – type of tissue and number of portions.

Sample set #	Type of tissue	N° of portions
1	colon	4
2	stomach	3
3	spleen	4
4	colon	3
5	stomach	3
6	colon	4
7	ileon	6
8	colon	4
9	colon	5
10	colon	2

formalin, a Cl concentration decrease of 94% and a K concentration decrease of 89% were determined. The behaviour of Ca (Fig. 3) concentration was variable for the different samples. Although remaining within the same average value for the different fixation times, for some sample sets (#1, #3, #6, and #7) the values both increased and decreased with time. On the other hand, P concentration increased in every sample set (Fig. 3), ranging from a 23% increase in sample #4, after eight days in formalin, to an increase of 66% in sample #1, after six days.

Regarding S, Fe, Cu, and Zn (Fig. 3), the behaviour is quite stable with time in formalin, with variations between samples that can be attributed to some variability and inhomogeneity within the tissue. Noteworthy is, again, the high values of Fe in sample set #3 (spleen). This is expected as spleen is one of the Fe reservoirs in the human organism.

The obtained results show that preservation and fixation for >2 days definitely alter the elemental concentration of K, Cl, and P. The decrease of K and increase of P were already determined by Chwiej et al. [31] for rat brain tissues perfused and immerse in 10% formalin solution. Conversely, no significant changes were observed for Zn, Cu, S, and Ca, whilst a great decrease of Cl was measured. The influence of formalin can explain the large range of values found in literature for K in the different organs, due to preservation or not in this solution. For instance, concentration of K in benign lung tissue was found to be $414 \pm 303 \mu\text{g/g}$, in a study by Kubala-Kukus et al. [35] where the samples were preserved in formalin between collection and preparation and evaluation. Similarly, Magalhães et al. [21] discovered significant differences in K content of adjacent normal healthy tissue and cancerous tissues from Portuguese patients (tissues preserved in formalin solution) and in German patients (cryo-preserved tissues).

Table 2
Elemental concentrations ($\mu\text{g/g}$) found in literature for colon, stomach, spleen, and other tissues.

	P	S	Cl	K	Ca	Fe	Cu	Zn	Ref.
colon	1020 \pm 270 to 7730 \pm 2350	2370 \pm 620 to 5110 \pm 850		210 \pm 90 to 1830 \pm 440	398 \pm 40 to 1340 \pm 480	51 \pm 23 to 260 \pm 26	5 \pm 2 to 28 \pm 4	33 \pm 10 to 100 \pm 10	[42]
stomach			5295 \pm 560	387 \pm 62	647 \pm 32	43.1 \pm 8.33	63.5 \pm 9.4	9.65 \pm 4.5	[3]
spleen	5460 to 3188.04 \pm 241.8	1953.6 \pm 122.88 to 2370		4034.16 \pm 253.5 to 5920	32.92 \pm 5 to 2070	185.19 \pm 41.61 to 547	1.107 \pm 0.069 to 1.9	16.98 \pm 1.23 to 159	[12]
	2852 \pm 564	10,756 \pm 1587		3839 \pm 415	2715 \pm 1207	173 \pm 55		699 \pm 221	[43]
other tissues	2210 \pm 120	295 \pm 120 to 3775 \pm 280		17 \pm 8 to 685 \pm 69	153 \pm 53 to 1590 \pm 90	5 \pm 2 to 66 \pm 7	2 \pm 1 to 35 \pm 5	6 \pm 3 to 74 \pm 7	[42]
	1000 to 8240		350 to 8200	100 to 3100		20 to 552	0.76 to 97	10 to 144	[15]
	4290 \pm 1578	8259 \pm 2002	3400 \pm 1452	6418 \pm 2625	1682 \pm 999	223 \pm 95	4.08 \pm 1.22	94.8 \pm 39.6	[44]

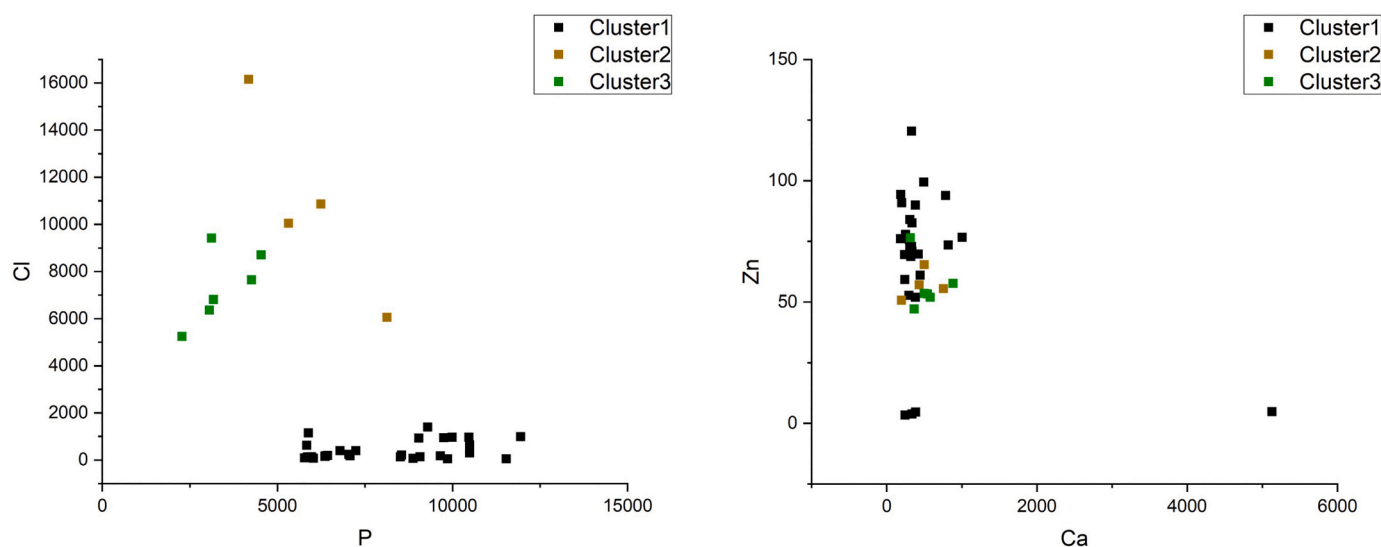


Fig. 4. K-means cluster analysis plots comparing Cl—P and Zn—Ca distances.

On the other hand, and in agreement with our findings, the research published by Majewska et al. [3] suffered no hindering when focusing on Cu, Fe and Zn in the comparison of malignant and benign breast, colon and lung tissues that were preserved in formalin.

Wróbel et al. [25] also determined a drastic decrease of K (a concentration over 140 times lower) content between freeze-dried tissue and corresponding mirrored sample after a paraffinization and deparaffinization process. In this study, the obtained concentration of Ca also showed variation while other elements, such as, Mn, Fe, Cu, and Zn showed no significant differences.

Following the presented results and to evaluate the migration of elements between formalin and tissue, the solutions in which each tissue (Table 1) was fixated were conserved and analysed as depositions in paper filter retainers.

Table S4 (Appendix) presents the results obtained for k-means cluster analysis rendering a 3-cluster distribution of the measured samples. In a first cluster are allocated all the tissue samples after formalin fixation, while snap-frozen lyophilized samples are distributed in two other clusters. Fig. 4 shows the k-mean cluster analysis plots comparing Cl—P and Zn—Ca distances. Remaining plots are presented in supplementary material (Fig. S3 (Appendix)). As can be seen, the elements responsible

for this clustering are P, Cl and K, while for elements such as Ca, S, Fe, Cu and Zn, the tissues present similar characteristics.

Fig. 5 shows the comparison of the elemental concentration of the filter retainer before and after the addition of 200 μL of fresh formalin. As can be seen, P concentration increases ($6000 \pm 300 \mu\text{g/g}$) after the addition of fresh formalin, when compared to the sterile paper filter. This could be due to the use of buffered formalin, important to stabilize the pH in the solution, typically using sodium phosphate. Regarding K and Cl, no alteration was verified.

Finally, using sample set #7 as the example for the longest time in formalin (24 days), Fig. 6 shows the variation of elemental concentration of paper filter deposited with formalin for different fixation times, compared to fresh formalin. As can be seen, there is a clear increase of Cl and K after tissue fixation, while the variation of the concentration of elements such as Fe, Cu, and Zn is not significant and could be a consequence of inhomogeneity of the paper filter. Regarding P, although a decrease could be expected, due to incorporation in the tissue, it was not observed likely because of the high-volume ratio formalin/tissue.

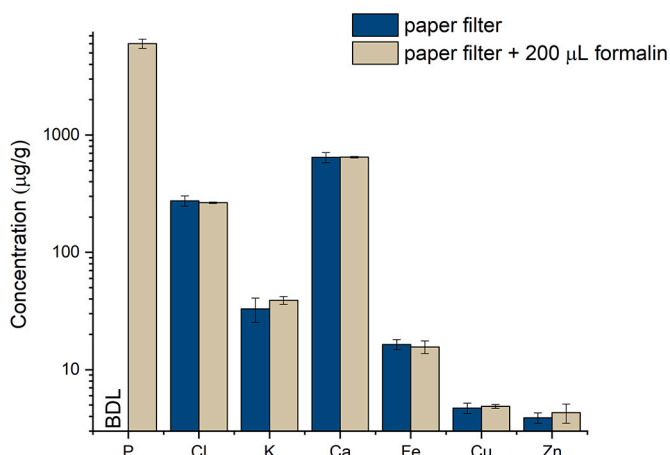


Fig. 5. Bar charts comparing the P, Cl, K, Ca, Fe, Cu and Zn mean elemental concentration ($\mu\text{g/g}$) of paper filter retainer before and after addition of 200 μL of fresh formalin. Error bars correspond to the quadratic sum of uncertainties - maximum deviation to the mean of two replica and maximum uncertainty determined by regression analysis.

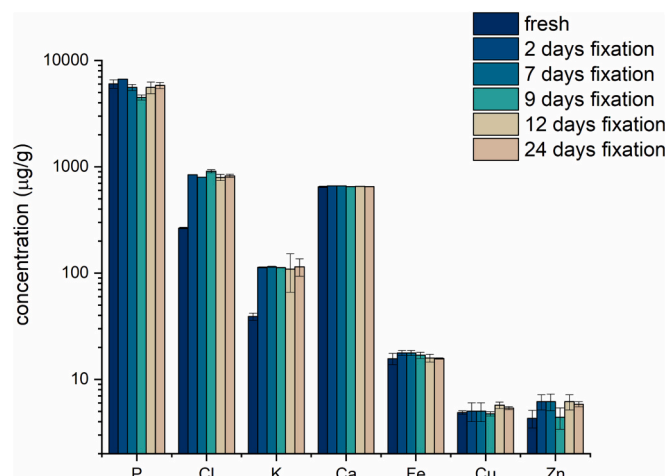


Fig. 6. Bar charts comparing the P, Cl, K, Ca, Fe, Cu and Zn mean elemental concentration ($\mu\text{g/g}$) paper filter retainer after addition of 200 μL of formalin with different fixation times (2, 7, 9, 12 and 24 days). Error bars correspond to the maximum deviation to the mean. Error bars correspond to the quadratic sum of uncertainties - maximum deviation to the mean of two replica and maximum uncertainty determined by regression analysis.

4. Conclusion

Formalin has an important place in biomedicine, as it is used in anatomy laboratories for long-term cadaver storage without decomposition, and in histology and pathology laboratories during the fixation stage of tissues. In this paper, we shed light on the limitations of formalin use and the influence on the elemental content of tissues. We determined the alterations induced by formalin in the elemental composition of tissues after fixation during different periods of time and how this should be taken into account when analysing tissues that have been stored in formalin or preserved as Formalin Fixed Paraffin Embedded blocks.

Taking into account that adjacent normal healthy tissue is not collected from patients lightly, we have evaluated the influence of formalin fixation time in the elemental composition of human tissue samples. Although the study could have gained from increased number of samples our results showed a clear decrease of Cl and K in the tissues, transferred to the formalin solution. Conversely, there is a P uptake from

the P present in formalin, likely due to the buffering solution. The consistent alterations seen in the studied elements across all the ten different tissues allow us to hypothesize that in the future, there will be different cut-offs for their diagnostic use in unfixed (intraoperative exams) and paraffin embedded tissue.

Future research is needed to investigate the elemental exchanges occurred before 48 h of fixation, so that thresholds for the influence of formalin fixation in human tissue can be established.

CRedit authorship contribution statement

Sofia Pessanha: Conceptualization, Methodology, Writing – original draft, Writing – review & editing. **Alexandre Veiga:** Formal analysis. **Delfim Douzel:** Resources, Methodology. **Fernanda Silva:** Resources, Methodology. **João Silva:** Formal analysis, Writing – original draft. **Patrícia M. Carvalho:** Data curation, Writing – original draft. **Sofia Barbosa:** Data curation, Writing – original draft, Writing – review & editing. **José Paulo Santos:** Supervision, Writing – original draft. **Ana Félix:** Supervision, Resources, Writing – original draft, Writing – review & editing. **Jorge Machado:** Conceptualization, Methodology, Writing – original draft.

Declaration of Competing Interest

There are no conflicts of interest.

Data availability

Data will be made available on request.

Acknowledgments

This work was partially supported by the research centre grant UID/FIS/04559/2021 to LIBPhys-UNL from the FCT/MCTES/PIDDAC, Portugal.

S. Pessanha and P. M. Carvalho acknowledge the support of FCT (Portugal) under contracts CEECIND/00278/2018 and PD/BD/128324/2017.

Appendix A. Supplementary data

Supplementary data to this article can be found online at <https://doi.org/10.1016/j.sab.2023.106704>.

References

- [1] T. Paunesku, M.B. Wanzer, E.N. Kirillova, K.N. Muksinova, V.S. Revina, E. R. Lyubchansky, B. Grosche, M. Birschwilks, S. Vogt, L. Finney, G.E. Woloschak, *Health Phys.* 103 (2012) 181–186.
- [2] M. Wołonciej, E. Milewska, W. Roszkowska-Jakimiec, Trace elements as an activator of antioxidant enzymes, *Postepy Hig. Med. Dosw.* 70 (2016) 1483–1498.
- [3] U. Majewska, D. Banaś, J. Braziewicz, S. Gózdź, A. Kubala-Kukus, M. Kucharzewski, *Phys. Med. Biol.* 52 (2007) 3895–3911.
- [4] O. Marques, B.M. da Silva, G. Porto, C. Lopes, *Cancer Lett.* 347 (2014) 1–14.
- [5] G.R. Monteith, D. McAndrew, H.M. Faddy, S.J. Roberts-Thomson, *Nat. Rev. Cancer* 7 (2007) 519–530.
- [6] P.J. Parsons, F. Barbosa, *Spectrochim. Acta B* 62 (2007) 992–1003.
- [7] A. Banas, W.M. Kwiatek, K. Banas, M. Gajda, B. Pawlicki, T. Cichocki, *J. Biol. Inorg. Chem.* 15 (2010) 1147–1155.
- [8] A. Ensina, P.M. Carvalho, J. Machado, M.L. Carvalho, D. Casal, D. Pais, J.P. Santos, A.A. Dias, S. Pessanha, *J. Trace Elem. Med. Biol.* 68 (2021), 126837.
- [9] P.M.S. Carvalho, S. Pessanha, J. Machado, A.L. Silva, J. Veloso, D. Casal, D. Pais, J. P. Santos, *Spectrochim Acta Part B* 174 (2020), 105991.
- [10] G. Luis, H. Silva, J. Silveira, V. Manteigas, A. Mata, D. Marques, A. Jesus, M. Fonseca, S. Pessanha, *J. Raman Spectrosc.* 50 (2018) 380–386.
- [11] S.B. Reddy, M.J. Charles, G.J.N. Raju, V. Vijayan, B.S. Reddy, M.R. Kumar, B. Sundareswar, *Nucl. Inst. Methods Phys. Res. B* 207 (2003) 345–355.
- [12] K. Planeta, A. Kubala-Kukus, A. Drozd, K. Matusiak, Z. Setkowicz, J. Chwiej, *Sci. Rep.* 11 (2021) 3704.
- [13] I.O. Farah, P.X. Nguyen, Z. Arslan, W. Ayensu, J.A. Cameron, Significance of differential metal loads in normal versus cancerous cadaver tissues, *Biomed. Sci. Instrum.* 46 (2010) 404–409.

- [14] A.M. Ebrahim, M.A.H. Eltayeb, M.K. Shaat, N.M.A. Mohamed, E.A. Eltayeb, A. Y. Ahmed, *Sci. Total Environ.* 383 (2007) 52–58.
- [15] A.N. Garg, V. Singh, R.G. Weginwar, V.N. Sagdeo, *Biol. Trace Elem. Res.* 46 (1994) 185–202.
- [16] J. Machado, P.M. Carvalho, A. Félix, D. Doutel, J.P. Santos, M.L. Carvalho, S. Pessanha, *J. Anal. At. Spectrom.* 35 (2020) 2920–2927.
- [17] G.E. Falchini, A. Malezan, M.E. Poletti, E. Soria, M. Pasqualini, R.D. Perez, *Radiat. Phys. Chem.* 179 (2021) 1–7.
- [18] S.J. Mulware, *J. Biophys.* 2013 (2013), 192026.
- [19] A.D. Surowka, P. Wrobel, D. Adamek, E. Radwanska, M. Szczerbowska-Boruchowska, *Metalomics* 7 (2015) 1522–1531.
- [20] D.O. Olaiya, O.I. Alatise, O.O. Oketayo, O.E. Abiye, E.I. Obianjunwa, F.A. Balogun, *Breast Cancer (Auckl.)* 13 (2019) 1–6.
- [21] T. Magalhães, M.L. Carvalho, A. von Bohlen, M. Becker, *Spectrochim. Acta Part B At Spectrosc.* 65 (2010) 493–498.
- [22] M.P. Silva, A. Tomal, A. Ribeiro-Silva, M.E. Poletti, *X-Ray Spectrom.* 38 (2009) 103–111.
- [23] F. le Naour, C. Sandt, C. Peng, N. Trcera, F. Chiappini, A.M. Flank, C. Guettier, P. Dumas, *Anal. Chem.* 84 (2012) 10260–10266.
- [24] A.G. Sarafanov, T.I. Todorov, A. Kajdacsy-Balla, M.A. Gray, V. Macias, J. A. Centeno, *J. Trace Elem. Med. Biol.* 22 (2008) 305–314.
- [25] P.M. Wróbel, L. Chmura, P. Kasprzyk, K. Kozłowski, K. Wątor, M. Szczerbowska-Boruchowska, *Spectrochim Acta Part B* 173 (2020), 105971.
- [26] A. Al-Ebraheem, K. Geraki, R. Leek, A.L. Harris, M.J. Farquharson, *X-Ray Spectrom.* 42 (2013) 330–336.
- [27] D. Schirotti, C. Marraccini, E. Zanetti, M. Ragazzi, A. Gianoncelli, E. Quartieri, E. Gasparini, S. Iotti, R. Baricchi, L. Merolle, *Diagnostics* 11 (2021) 727.
- [28] L. Pascolo, A. Gianoncelli, C. Rizzardi, V. Tisato, M. Salomé, C. Calligaro, F. Salvi, D. Paterson, P. Zamboni, *Sci. Rep.* 4 (2014) 6540.
- [29] L. Pascolo, A. Gianoncelli, G. Schneider, M. Salomé, M. Schneider, C. Calligaro, M. Kiskinova, M. Melato, C. Rizzardi, *Sci. Rep.* 3 (2013) 1123.
- [30] E.M. Johnston, E. Dao, M.J. Farquharson, *X-Ray Spectrom.* 48 (2019) 432–437.
- [31] J. Chwiej, M. Szczerbowska-Boruchowska, M. Lankosz, S. Wojcik, G. Falkenberg, Z. Stegowski, Z. Setkowicz, *Spectrochim Acta Part B* 60 (2005) 1531–1537.
- [32] R. Quester, R. Schröder, *J. Neurosci. Methods* 75 (1997) 81–89.
- [33] D.E.B. Fleming, S.L. Crook, C.T. Evans, M.N. Nader, M. Atia, J.M.T. Hicks, E. Sweeney, C.R. McFarlane, J.S. Kim, E. Keltie, A. Adishes, *Appl. Radiat. Isot.* 167 (2021), 109491.
- [34] R. Zhang, L. Li, Y. Sultanbawa, Z.P. Xu, *Am. J. Nucl. Med. Mol. Imaging* 8 (2018) 169–18835.
- [35] A. Kubala-Kukus, J. Braziewicz, D. Banas, U. Majewska, S. Gózdź, A. Urbaniak, *Nucl. Inst. Methods Phys. Res. B* 150 (1999) 193–199.
- [36] R. Sitko, B. Zawisza, *Quantification in X-ray fluorescence spectrometry*, in: K. Shatendra (Ed.), *X-Ray Spectrometry*, Sharma, InTech, 2012.
- [37] J. Sherman, *Spectrochim. Acta* 7 (1955) 283–306.
- [38] R. Van G.E. Marguif, *X-Ray Fluorescence Spectrometry and Related Techniques: An Introduction*, Momentum Press, New York, 2013.
- [39] S. Pessanha, E. Marguif, M.L. Carvalho, I. Queral, *Spectrochim Acta Part B* 164 (2020), 105762.
- [40] M. Manso, S. Pessanha, M. Guerra, J.L. Figueirinhas, J.P. Santos, M.L. Carvalho, *Spectrochim Acta Part B* 130 (2017) 35–38.
- [41] M. Manso, S. Pessanha, M.L. Carvalho, *Spectrochim Acta Part B* 61 (2006) 922–928.
- [42] T. Magalhães, A. von Bohlen, M.L. Carvalho, M. Becker, *Spectrochim Acta Part B* 61 (2006) 1185–1193.
- [43] R.G. Leitão, A. Palumbo, P.A.V.R. Souza, G.R. Pereira, C.G.L. Canellas, M.J. Anjos, L.E. Nasciutti, R.T. Lopes, *Radiat. Phys. Chem.* 95 (2014) 62–64.
- [44] V. Zaichick, S. Zaichick, *J. Cancer Metastasis Treat.* 4 (2018) 60.